Volume 4, Number 1 (March, 2011) p. 100 - 122 • ISSN 1983-4195

IBRACON

REVISTA IBRACON DE ESTRUTURAS E MATERIAIS
IBRACON STRUCTURES AND MATERIALS JOURNAL

Shear strength mechanisms in reinforced concrete structures: a one-dimensional finite element approach

Mecanismos de resistência ao cisalhamento em estruturas de concreto armado: uma abordagem via método dos elementos finitos unidimensionais



C. G. NOGUEIRA [a]
gorlanog@sc.usp.br

H. B. CODA [b]
hbcoda@sc.usp.br

W. S. VENTURINI [c]
venturin@sc.usp.br

Abstract

This paper shows the development of a mechanical model to reinforced concrete analysis based on the finite element method, taking into account the non-linear material behavior with shear strength mechanisms, such as shear reinforcement and dowel action. These mechanisms are coupled to a damage model for concrete to better represent the material stiffness loss, as well as the global response of beams. Numerical examples are presented to validate the model, verifying the importance of these contributions, mainly for hyperstatic beams with high span-to-depth ratio.

Keywords: Finite element method, damage, complementary mechanisms, shear strength, beams.

Resumo

Este trabalho apresenta um modelo mecânico para análise de vigas em concreto armado com base no método dos elementos finitos, considerando a não-linearidade física dos materiais em conjunto com mecanismos específicos de resistência ao cisalhamento do concreto armado, tais como a armadura transversal e o efeito de pino. Esses mecanismos são acoplados a um modelo de dano para o concreto com o objetivo de representar melhor as perdas de rigidez do material, bem como a resposta global das vigas. Foram apresentados exemplos numéricos para validação do modelo, verificando-se a importância dessas contribuições, principalmente em vigas hiperestáticas com elevada relação altura/comprimento.

Palavras-chave: Método dos elementos finitos, dano, mecanismos complementares, resistência ao cisalhamento, vigas.

[a] *Escola de Engenharia de São Carlos, Departamento de Engenharia de Estruturas, Universidade de São Paulo, Pós-doutorando, gorlanog@sc.usp.br, Av. Trabalhador Sãocarlense 400, CEP 13560-000, São Carlos-SP, Brasil;*
[b] *Escola de Engenharia de São Carlos, Departamento de Engenharia de Estruturas, Universidade de São Paulo, Professor associado, hbcoda@sc.usp.br, Av. Trabalhador Sãocarlense 400, CEP 13560-000, São Carlos-SP, Brasil;*
[c] *Escola de Engenharia de São Carlos, Departamento de Engenharia de Estruturas, Universidade de São Paulo, Professor titular, venturin@sc.usp.br, Av. Trabalhador Sãocarlense 400, CEP 13560-000, São Carlos-SP, Brasil.*

Received: 27 Oct 2010 • Accepted: 03 Jan 2011 • Available Online: 04 Mar 2011

1. Introduction

Although the modeling of reinforced concrete structures is well developed, nowadays there is not a complete mathematical model able to describe, with great accuracy, the response of reinforced concrete and its several mechanisms of stress transferring. Its non-linear behavior is a direct function of concrete cracking and steel yielding, which are responsible for the occurrence of other phenomena such as: tension stiffening, aggregate interlock, dowel action and bond-slip behavior between steel and the surrounding concrete. In literature, there are many scientific studies that seek to identify and quantify these phenomena, such as the works of Krefeld and Thurston [1], Dei Poli et al. [2], Gergely [3], Dulacska [4], Jimenez et al. [5], Walraven [6], Laible et al. [7], Bazant and Gambarova [8], Millard and Johnson [9]. In this paper, the main objectives are to study the shear strength mechanisms developed in reinforced concrete members. The adopted theoretical basis is the Ritter-Mörsch truss analogy. The compression struts that develop along the inclined plane of cracking provide a portion of concrete shear strength contribution, while the vertical ties guarantee the shear reinforcement contribution. The concrete portion contains the so-called complementary mechanisms of shear strength, defined by the aggregate interlock and the dowel action. The current structural design codes provide expressions for calculating the overall concrete portion of the member strength as a function of its compressive strength and geometric dimensions, however nothing is mentioned regarding complementary mechanisms. The shear reinforcement, on its turn, is calculated in order to absorb the excess of shear force that is not resisted by the concrete. Then, the main challenge is to adequately represent how these stress transfers occur in the aggregates, through the longitudinal reinforcement, which works as a dowel, and from the cracked concrete to the shear reinforcement, so that these effects can be incorporated in numeric models (Martín-Perez and Pantazopoulou [10], He and Kwan [11], El-Ariss [12], Sanches Jr and Venturini [13], Oliver et al. [14]). Thus, this paper aims to present a mechanical model for the analysis of reinforced concrete taking into account, beyond the non-linear behavior of steel and concrete, complementary shear strength mechanisms. For this purpose, the strength portions of the shear reinforcement and dowel action are incorporated into a one-dimensional finite element computational code through approximate models. Since the behavior of the shear reinforcement and the dowel action is directly connected to the intensity of the cracking/degradation of the concrete, these effects are coupled to the damage model. Thus, the developed mechanical model is interesting in two ways: the first one is the improvement of numerical modeling because it takes into account all these complementary shear effects and the second one concerns the computational processing efficiency because it is implemented in a one-dimensional finite element.

2. Proposed mechanical model

2.1 One-dimensional FEM with Timoshenko's theory

The Euler-Bernoulli's hypothesis for bending of beams takes into account that the strains caused by shear stress are zero throughout the entire cross section. Such consideration can be adopted in beams whose length is much larger than its height. However, when it comes to deep beams, the effect of shear strain, given by Timoshenko's theory, cannot be neglected. The fundamental hypothesis of Timoshenko's theory considers that the plane cross sections remain plane after strain, but no more orthogonal to the element axis, which gives a better representation of the problem. Such consideration leads to an increase in the curvature of the cross sections, which means a new contribution on the energy functional of the problem, added to the of pure bending moment energy. Including this energy, the member stiffness is reduced, causing a displacement increase. Several authors proposed finite elements that incorporated Timoshenko's hypothesis, such as Nickel and Secor [15], Prathap and Bhashyam [16] and Heyliger and Reddy [17]. The formulations differ only in the choice of interpolating functions to approximate the transversal displacements and rotations. In this work, third and second degree polynomials are used to approximate transversal displacements and rotations, respectively. The nodal parameters are the total displacements (v_1 and v_2) that correspond to the contributions of bending moment and shear force, as well as the rotation (ϕ_1 and ϕ_2) generated only by the bending moment, since both quantities are continuous throughout the length of the element. The distortions are calculated with proper parameters and added to the bending moment rotations to constitute the total rotation of the extremity of the finite elements. Figure 1 shows the adopted beam finite element. The stiffness matrix of the Timoshenko's finite element, obtained from the minimization of total potential energy functional, is given by equation (1):

Figure 1 – Finite element adopted

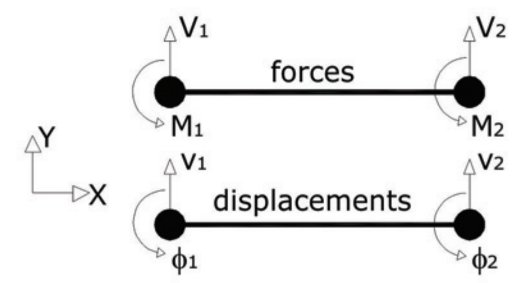

$$[K]=\frac{EI}{1+2g}\begin{bmatrix} \frac{12}{L^3} & \frac{6}{L^2} & \frac{-12}{L^3} & \frac{6}{L^2} \\ \frac{6}{L^2} & \frac{2}{L}(2+g) & \frac{-6}{L^2} & \frac{2}{L}(2-g) \\ \frac{-12}{L^3} & \frac{-6}{L^2} & \frac{12}{L^3} & \frac{-6}{L^2} \\ \frac{6}{L^2} & \frac{2}{L}(2-g) & \frac{-6}{L^2} & \frac{2}{L}(2+g) \end{bmatrix} \quad (1)$$

in which: *L* is the finite element length; *g* is the Weaver's constant that takes into account the influence of the shear strains given by $6E/kGAL^2$; *E* and *G* are, respectively, the longitudinal and transversal elasticity modulus of the concrete; *I* is inertia moment of the cross section; *A* is the area of the cross section; *k* is the form factor of the cross section, which for rectangular sections is equal to 0.8333.

2.2 Material non-linearity for concrete

From the mechanical perspective, the cracking degrades the material stiffness reflecting directly in his structural response. Thus, the damage mechanics is an interesting theory to model the stiffness loss in concrete because it quantifies the intensity of the material degradation as the load is applied. The Mazars's damage model [18] is adopted, in which the damage is caused only by the presence of elongations caused by tensile strains. The damage is represented locally by a scalar variable *D*, which can vary from 0 to 1. Damage equal to zero represents a state of complete integrity of the material, while damage equal to one represents a state of complete degradation of the material. The criteria for verifying the existence of damage in a specific point of the material is defined by equation (2):

$$f(\tilde{\varepsilon}, D) = \tilde{\varepsilon} - \hat{S}(D) \leq 0 \quad (2)$$

$$\tilde{\varepsilon} = \sqrt{(\varepsilon_1)_+^2 + (\varepsilon_2)_+^2 + (\varepsilon_3)_+^2} \quad (3)$$

in which: $\tilde{\varepsilon}$ is a measure of equivalent strain that represents the elongation state at a point; $\hat{S}(D)$ is the reference strain which is updated based on the damage level; $(\varepsilon_i)_+$ represents the positive components of the main strains tensor.

Figure 2 – Nonlinear behavior for the steel

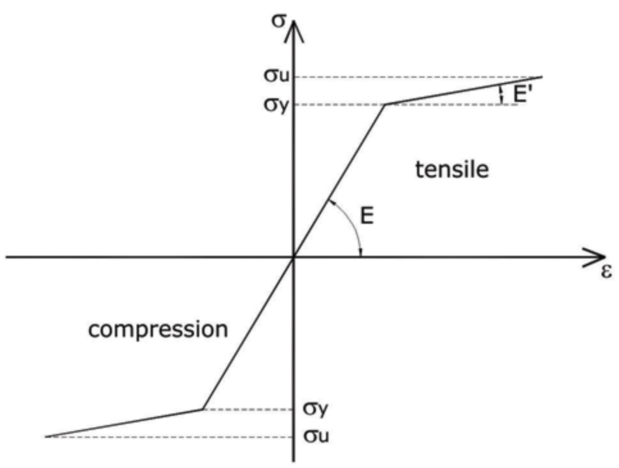

The damage variable is calculated as a function of the strain state of each point, as well as in terms of an internal set of parameters. These parameters are calibrated from the experimental stress-strain relations for tension and compression in concrete specimens (Sanches Jr and Venturini [13], Nogueira [19]). Therefore, the normal and shear stresses evolution are obtained by the incremental Hooke's law penalized by the damage variable according to:

$$\dot{\underline{\sigma}} = (1 - D)\underline{\underline{D}}_0 \cdot \dot{\underline{\varepsilon}} \quad (4)$$

in which: $\underline{\sigma}$ and $\underline{\varepsilon}$ are, respectively, the second order tensors of stress and strain at each integration point; *D* is the damage variable; $\underline{\underline{D}}_0$ is the fourth order tensor of the material elastic properties. Details on damage mechanics and its formulations can be found in Kachanov [20], Lemaitre and Chaboche [21], Botta [22], Pituba [23], Paula [24], Álvares [25], Araújo [26].

2.3 Material non-linearity for steel

The nonlinear behavior of steel is defined by its yielding observed when the stress level is larger than a reference value. Movements arise between crystals of the material without loss of cohesion or internal breaking, eliminating the elastic behavior. Therefore, plasticity theory becomes appropriate to describe steel. Details on the formulations can be found in Owen and Hinton [27] and Proença [28]. The utilized model in this work considers steel with positive linear isotropic hardening resulting in a bi-linear constitutive law, according to figure 2. The yielding criteria can be written in the following manner:

$$f^{i+1} = \sigma^{i+1} - (\sigma_y + K\alpha^{i+1}) \leq 0 \quad (5)$$

Thus, the stress in the reinforcement is calculated according to the following incremental relation:

$$\begin{aligned} f^{i+1} < 0 &\rightarrow \dot{\sigma}^{i+1} = E\dot{\varepsilon}^{i+1} \\ f^{i+1} \geq 0 &\rightarrow \dot{\sigma}^{i+1} = E_a\dot{\varepsilon}^{i+1} \end{aligned} \quad (6)$$

in which: E_a is the actual steel longitudinal elasticity module given by $E_a = EK/(E+K)$; σ^{i+1} is the steel stress in the next iteration; σ_y is the steel reference yielding stress; *K* is the steel positive isotropic hardening parameter; α^{i+1} is a measure of the plastic strain updated in every iteration; *E* is the steel initial longitudinal elasticity module; ε^{i+1} is the total strain in the next iteration.

2.4 Transversal reinforcement contribution (V_{sw})

The shear reinforcement begins to be effectively stressed after the beginning of the concrete cracking, which on its turn, comes from the damage evolution (Belarbi and Hsu [29]). Due to this reason, the proposed model to simulate the presence of a shear reinforcement is directly associated with the concept of concrete damage. Therefore, the criterion through which the stirrups are stressed is defined by the damage criterion, established by equation (2). It is admitted that after the beginning of the damaging, the main strain tensor can be decomposed in an elastic portion (*e*) and in another portion dissipated by damage (*d*):

$$\underline{\varepsilon} = \underline{\varepsilon}^{e} + \underline{\varepsilon}^{d} \tag{7}$$

Extending the same principle for the stress tensor, one can conclude that:

$$\underline{\sigma} = (1 - D)\underline{\underline{D}}_0 \cdot \underline{\varepsilon} \rightarrow \underline{\sigma} = \underline{\underline{D}}_0 \cdot \underline{\varepsilon} - D\underline{\underline{D}}_0 \cdot \underline{\varepsilon} \tag{8}$$

$$\underline{\sigma}^{d} = D\underline{\underline{D}}_0 \cdot \underline{\varepsilon} \rightarrow \underline{\varepsilon}^{d} = D\underline{\varepsilon} \tag{9}$$

Therefore, equation (9) provides the strain portion, ε^d, which must be absorbed by the shear reinforcement, while the non-dissipated portion is absorbed by the concrete. Therefore, the damage model defines the contribution of the concrete on the shear force strength, and transfers part of the dissipated portion due to the loss of stiffness, which comes from cracking, to the shear reinforcement. The dissipated strain portion is defined at each integration point along the cross sections of the finite element and follows the same direction defined by the main tensile strain. As the stirrups are positioned in the vertical, it is necessary to obtain the vertical components of this strain. Figure 3 illustrates the adopted procedure and the equation (10) presents the maximum value of the stirrups strain, neglecting compression.

$$\varepsilon_{sw} = \max\left[\varepsilon_1 D sen(\alpha)\right] \tag{10}$$

in which: ε_1 is the main tensile strain; *D* is the damage value; α is the main direction of tension. All of these quantities are defined at each integration point along the height of the cross sections of the finite elements. After, determining the strain in shear reinforcement, the transmitted force to each stirrup is given by the product $\sigma_{sw}A_{sw}$, which according to Ritter-Mörsch's truss analogy, can be considered for a width range equal to the effective height of the cross section. Thus, one defines the shear force portion transferred to the shear reinforcement according to:

$$V_{sw} = \sigma_{sw}\rho_{sw}b_w d \tag{11}$$

in which: ρ_{sw} is the shear reinforcement rate of each finite element defined by A_{sw}/sb_w ; *s* is the spacing between the stirrups; b_w is the width of the cross section; d is the effective height of the cross section; σ_{sw} is the stress in the stirrups obtained by the elastoplastic model defined in the item 2.3.

2.5 Dowel action contribution (V_d)

The bars that compose the longitudinal reinforcement contribute in the shear strength through the complementary mechanism known as dowel action. It is a reaction force that arises from the attempt of locally cutting and bending the reinforcement bars, when these are intercepted by a crack, as one can observe on figure 4. The hypothesis of a beam over an elastic base is adopted in order to

Figure 3 – Scheme for shear reinforcement vertical strain assessment

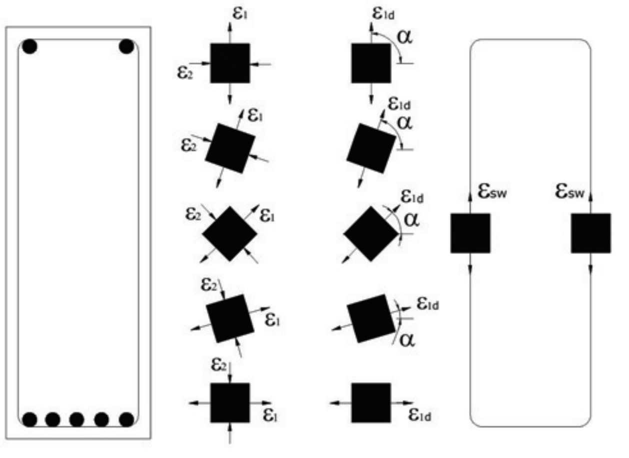

Figure 4 – Scheme for dowel action acting

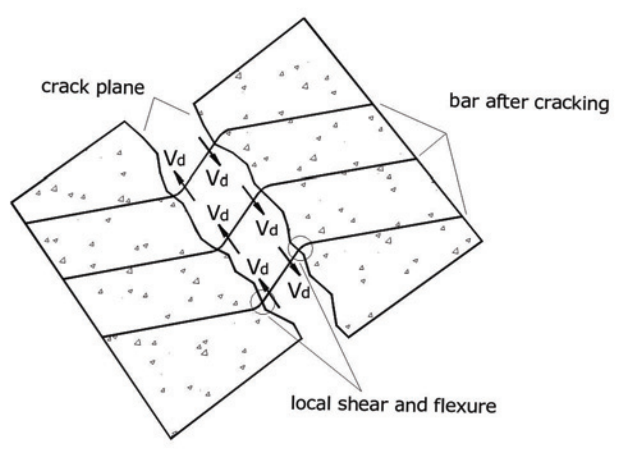

Figure 5 – Beam under elastic foundation hypothesis to simulate dowel action

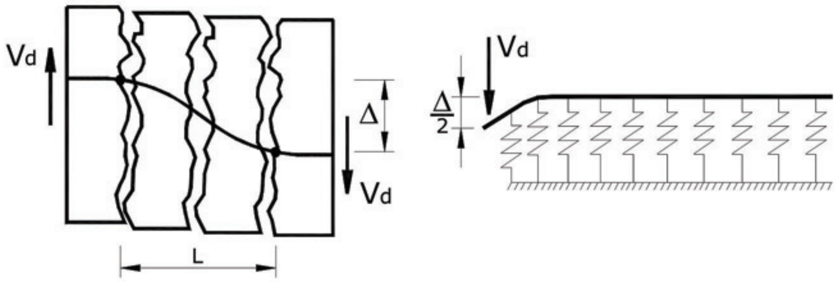

formulate the dowel action, where the longitudinal reinforcement bars are considered as supported beams over a deformable concrete base, as illustrated in figure 5. Thus, the dowel force can be written as:

$$V_d = K_d \Delta \quad (12)$$

in which: K_d is the stiffness of the concrete base; Δ is the dowel displacement undergone by the reinforcement. The length *L*, as depicted in figure 5, represents how much of the bar is subjected to the dowel displacement, therefore being able to be determined by relation π/λ. The parameter λ represents the relative stiffness of the foundation, defined by the concrete cover, according to:

$$\lambda = \sqrt[4]{\frac{k_c \phi_s}{4 E_s I_s}} \quad (13)$$

in which: k_c is the foundation module for the concrete cover; ϕ_s is the diameter of the equivalent bar correspondent to the total area of a reinforcement layer; E_s is the elasticity module of steel; I_s corresponds to the moment of inertia of the bar, which in the case of circular bars is given by $\pi\phi_s^4/64$. Soroushian et al. [30] proposed, from experimental tests, an expression to the concrete cover foundation module assessment:

$$k_c = \frac{127 c_1 \sqrt{f_c}}{\sqrt[3]{\phi_s^2}} \quad (14)$$

in which: f_c is the compression concrete strength given in N/mm²; c_1 is a coefficient that varies from 0.6 to 1.0. Thus, the dowel displacement can be obtained by the following expression:

$$\Delta = DL\left[\varepsilon_1 \cos(\alpha)\, sen(\alpha) + \gamma_{XY} \cos^2(\alpha)\right] \quad (15)$$

in which: α is the main tension direction defined with the horizontal plane; γ_{XY} is the distortion in each integration point.
The dowel stiffness value based on the area of a reinforcement layer is, then, defined by:

$$K_d = \frac{4A_s}{\pi\phi_s^2} E_s I_s \lambda^3 \quad (16)$$

After the stiffness calculation for every reinforcement layer, one obtains the dowel stresses at each integration point along the cross section of the finite element.

$$\tau_d = \begin{cases} \dfrac{4\rho_s E_s I_s \lambda^3 \Delta}{\pi\phi_s^2} \rightarrow \sigma_c \le f_c \;\; and \;\; \sigma_s \le f_s \\ \dfrac{1{,}27\rho_s \phi_s^2 \sqrt{f_c f_s}}{A_s} \rightarrow \sigma_c > f_c \;\; or \;\; \sigma_s > f_s \end{cases} \quad (17)$$

in which: ρ_s and A_s are, respectively, the longitudinal reinforcement rate and the total area of the reinforcement for each finite element; f_s is the steel yielding stress; σ_s and σ_c are, respectively, the acting stresses in the reinforcement and the concrete.
In case of the compressive concrete strength or steel yielding stress of any reinforcement layer is reached, the dowel action is limited by the given value of the second line of the equation (17). From the values of the dowel stress τ_d to each integration point along the element height, one integrates on the element length and obtains the shear force corresponding to the dowel action contribution to each finite element. As the damage increases at the integration points, their contribution to the dowel action also increases, so at the end of the loading process, all the dowel force compatible with the state of strain is mobilized.

2.6 Solution of the non-linear problem

In this work, the Newton-Raphson's technique with tangent stiffness matrix is used to solve the non-linear problem. The internal forces were calculated by integration of stresses over the finite elements, which were obtained by the respective models as described before:

$$N = \int_A \sigma_c dA + \sum_{i=1}^{cam} (\sigma_s A_s)_i$$
$$V = \int_A \tau_c dA + \int_A \tau_{d,\alpha} dA + \sigma_{sw} \rho_{sw} b_w d \quad (18)$$
$$M = \int_A \sigma_c y dA + \sum_{i=1}^{cam} (\sigma_s A_s y)_i$$

in which: $\int_A \tau_{d,\alpha} dA$ and $\sigma_{sw} \rho_{sw} b_w d$ are, respectively, the contributions of the dowel action and shear reinforcements; *y* is the distance from the integration point (or reinforcement layer) to the gravity center of the cross section; *cam* is the number of the reinforcement layers along the cross section; σ_c and τ_c are, respectively, the normal and tangential stresses on the concrete corrected by the damage model. The Gauss-Lobatto's numerical integration scheme, described by the figure 6, divides the domain in several integration points including its extremity and the middle point (Nogueira [19]). Therefore, the corrections, in order to consider dowel action and shear reinforcement contributions are introduced on the nodal force vector, by the values of the shear force calculated by the proposed models. So, if the shear strength of the cross section, given by equation (18), is smaller than the applied shear force, the obtained residue must be reapplied in the structure during the iterative process.

3. Results and discussion

3.1 Exemple 1

This beam was tested on the Laboratory of Structures of EESC-USP. The "I" cross section is approximated by a rectangular equivalent cross section, with a fixed height of 30.0cm as in the real section (SR). In the first case, the cross section width was calculated keeping the moment of inertia constant (BI) and after that, keeping the area constant (BA). Figure 7 shows the real and approximate geometric characteristics of the cross section, as well as the geometry of the beam and the applied load. The parameters used in the analysis are: concrete elasticity module 29632MPa; concrete Poisson's ratio 0.2; steel yielding stress 500MPa; steel elasticity module 177890MPa; steel hardening 17789MPa; concrete cover of the longitudinal reinforcement 1cm; 12 load steps; force and displacement tolerance 10^{-4}; 20 Gauss points for height; 6 Gauss points for length. The Mazars's damage parameters are: ε_{d0} = 0.000065; A_T = 0.914; B_T = 10390; A_C = 0.975; B_C = 1246 and the beam was discretized into a 30 longitudinal finite elements of same length. The equilibrium trajectory at the middle span is depicted in figure 8. Since for this problem flexure is predominant, the BI model response presents better results than the BA model, when both are compared to the experimental curve. Figure 9 illustrates the evolution of the stirrups strain of section AA. It is verified that the response obtained with the BI approximation is better than the BA response. In the test, the shear reinforcement began to be stressed after 30kN of loading. The mechanical model with approximation BI shows that the stirrups began to be significantly stressed after 30kN, which allows us to conclude that the shear reinforcement contribution criterion, based on the damage mechanical model for concrete, is well formulated.

3.2 Exemple 2

A clamped-clamped reinforced concrete beam, subjected to four concentrate loads is analyzed, as depicted in the figure 10. This beam was studied by Neves [31], who used 10 finite elements, Mazars's damage model for concrete and shear force transferred to the stirrups equal to the non-absorbed portion by the concrete, that is, $V_{sw} = V_{elastic} - V_{concrete}$. This hypothesis considers an elastic-linear behavior to the stirrups and no residues in shear force. The parameters used in the analysis are: concrete elasticity module 29200MPa; concrete Poisson's ratio 0.2; steel yielding stress 500MPa; steel elasticity module 196000MPa; steel hardening module 19600MPa; 12 load steps; force and displacement tolerance 10^{-4}; 22 Gauss points for height; 7 Gauss points for length. The adopted parameters to Mazars' damage model are: ε_{d0} = 0.000065; A_T = 0.910; B_T = 10390; A_C = 0.977; B_C = 1270. The analysis are made taking into account three mechanical models: Euler-Bernoulli (B),

Figure 6 – Cross section discretization and numerical integration scheme

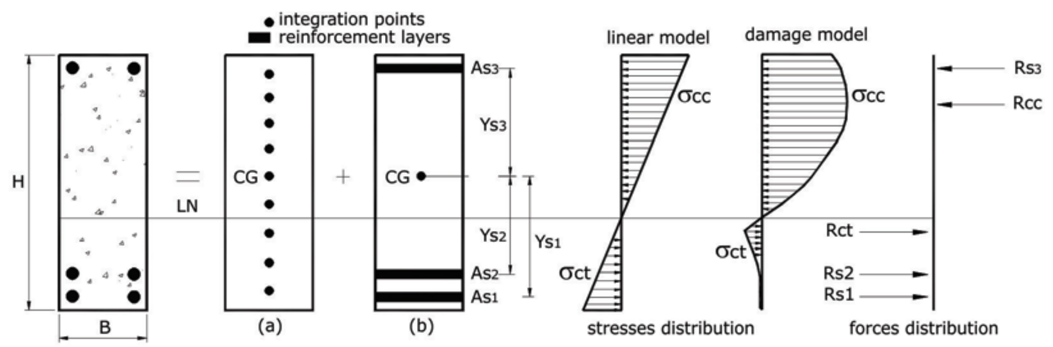

Figure 7 – Geometry, dimensions and applied loads for example 1

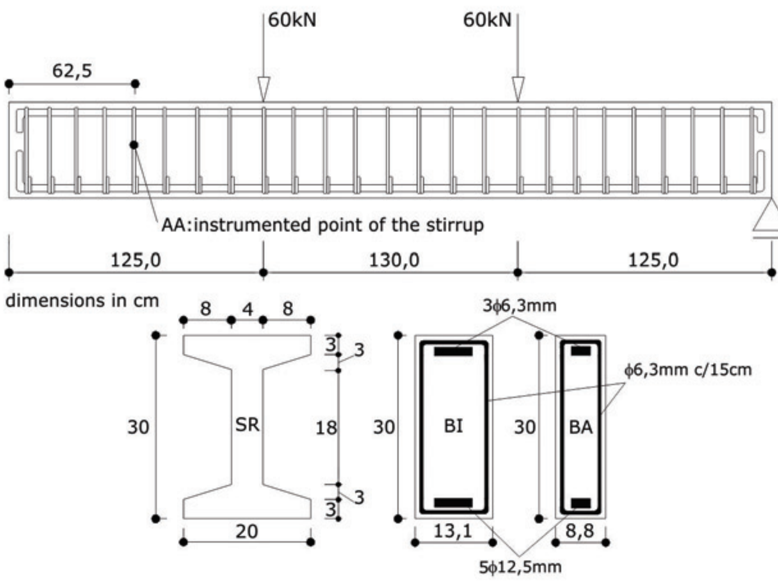

Timoshenko (T) and complete Timoshenko (TSD), that is, with shear reinforcement and dowel action. It is considered five different meshes: 10, 20, 40, 80 and 100 finite elements with same length. Figure 11 illustrates the convergence history using the middle span transversal displacement in the last load step as the verification criterion. The numerical stability of the response is achieved after 80 elements. Therefore, the study is performed with the mesh of 80 finite elements. Figure 12 presents the equilibrium trajectory of the middle span node. It is possible to observe a significant difference between the responses of T and TSD models when compared with the B model, because there is an important influence of the shear distortions (1.0/3.3 span-to-depth relation). In the final load steps, one can observe significant differences between T and TSD models in function of the dowel action and shear reinforcement contributions. The redundancy of the structure, with stresses redistribution, detached the complementary mechanism importance. In the figure 13 one can observe the stiffness loss in the left clamped cross section due to the total loading. With the contributions of the shear reinforcement and dowel action, less stiffness loss is verified as part of the concrete damaging is transferred these complemen-

Figure 8 – Equilibrium trajectory of the middle span point of the beam

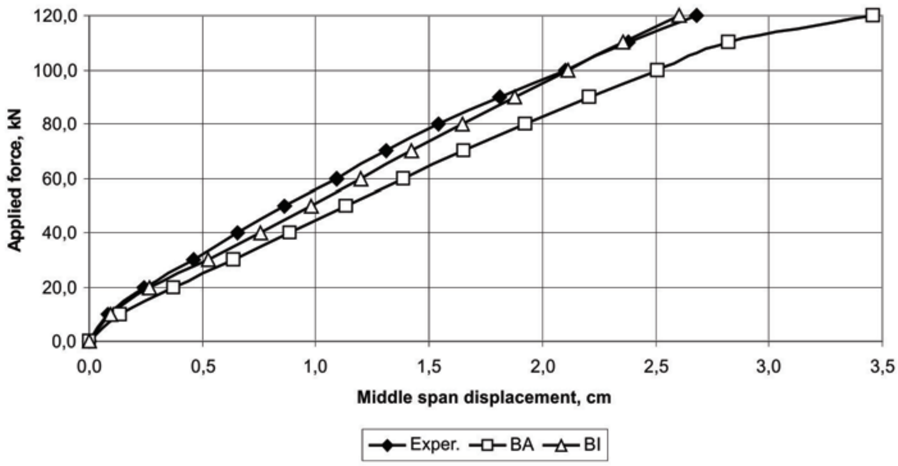

Figure 9 – Stirrup strain at AA section

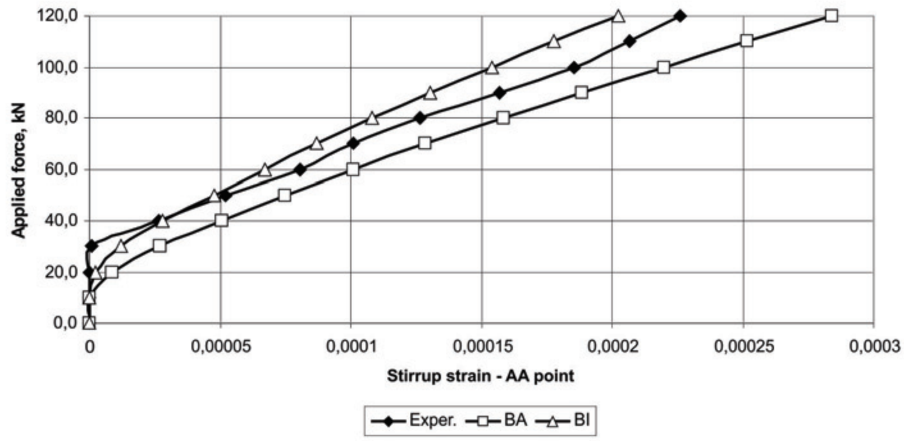

Figure 10 – Geometry, dimensions and applied loads for example 2

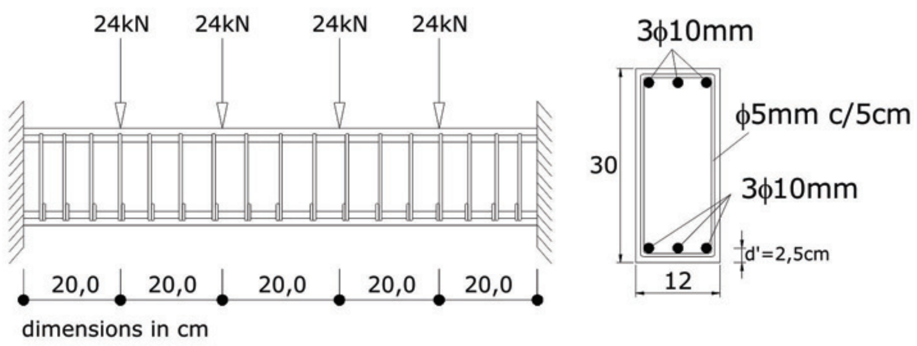

Figure 11 – Convergence analysis for the B, T and TSD models

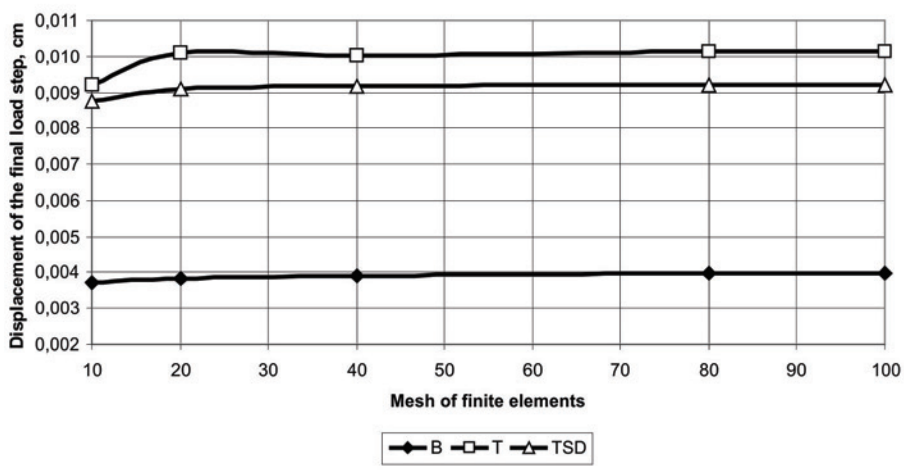

Figure 12 – Equilibrium trajectory of the middle span node: mesh of 80 finite elements

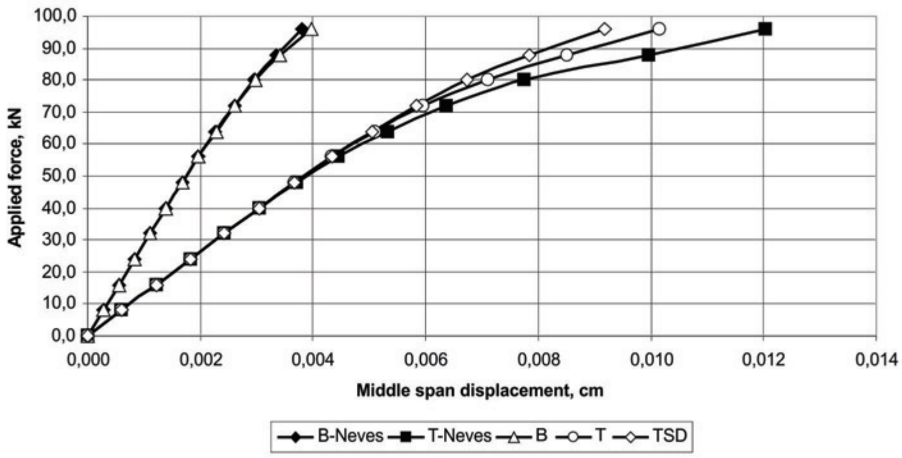

Figure 13 – Stiffness evolution of the left clamped cross section: mesh of 80 finite elements

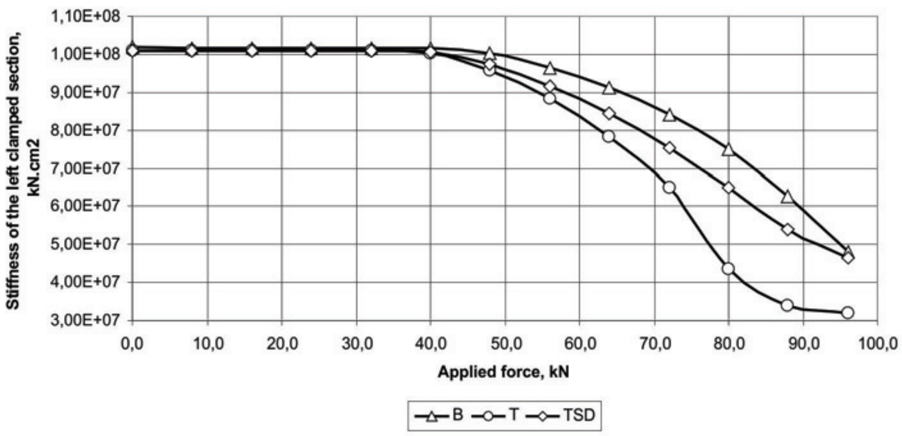

tary mechanisms. Another important item to be discussed is the stiffness variation due to the adopted discretization, as depicted in figures 14 and 15. Less refined meshes, in hyperstatic structures, tend to not represent properly these losses of stiffness, especially when shear effects are taken into account. The results of the 80 and 100 finite elements meshes were very close, thus consolidating the discretization choice. The larger redistribution observed in the T model when compared with B model comes from the bi-axial strain state. However, the TSD model guaranties less global stiffness loss of the structure at the end of analysis.

4. Conclusions

This work presents a mechanical model for bar finite elements that incorporates, in its formulation, the shear reinforcement and dowel effects, from basic concepts of damage mechanics. The main advantage of the model is to allow the consideration of shear strength mechanisms in a simple one-dimensional finite element, avoiding complete two-dimensional analyses of reinforced concrete beams. The criterion for the beginning of the stirrups stressing proved to be coherent with the experimental results, as observed in example 1. Another interesting aspect is the verification of the correlation between shear strength mechanisms and the span-to-depth relation of the beams, that is, the effects of the developed shear strength models are directly proportional to the span-to-depth ratio. The introduction of the shear strains mechanisms in the equilibrium of the structure allows understanding the smaller stiffness losses obtained with the TSD numerical model at the end of non-linear analysis. With respect to the processing time, using a computer with two 2.0GHz processors and 3GB of memory, the example 2 for 100 finite elements and the TSD formulation takes 8.7 minutes. All the other analyses presented an inferior processing time in comparison with the aforementioned value.

5. Acknowledgements

The authors would like to thank FAPESP – São Paulo Research Foundation for the finantial support. A special thank to Professor Wilson Sergio Venturini (in memoriam).

6. References

[01] KREFELD, W.J.; THURSTON, C.W. Studies of the shear and diagonal tension strength of simply supported reinforced concrete beams. ACI Journal, v.63, n.4, 1966; p.451-476.

[02] DEI POLI, S.; DI PRISCO, M.; GAMBAROVA, P.G. Shear response, deformations and subgrade stiffness of a dowel bar embedded in concrete. ACI Structural Journal, v.89, n.6, November-December, 1992; p.665-675.

[03] GERGELY, P. Splitting cracks along the main reinforcement in concrete members. Dept. of Structural Engineering, Report, Cornell University, 1969.

[04] DULACSKA, H. Dowel action of reinforcement crossing cracks in concrete. ACI Journal, Proceedings, v.69, n.12, December, 1972; p.754-757.

[05] JIMENES, R.; WRITE, R.N.; GERGELY, P. Bond and dowel capacities of reinforced concrete. ACI Journal, January, 1979; p.73-91.

[06] WALRAVEN, J.C. Fundamental analysis of aggregate interlock. Journal of the Structural Division, ASCE, v.107, n.ST11, November, 1981; p.2245-2270.

[07] LAIBLE, J.P.; WHITE, R.N.; GERGELY, P. Experimental investigation of seismic shear transfe

Figure 14 – Stiffness of the left clamped cross section × discretization: T model

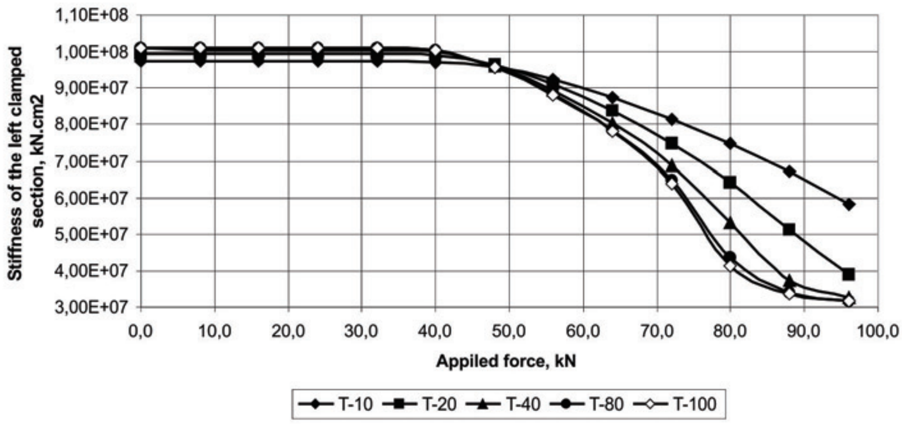

Figure 15 – Stiffness of the left clamped cross section × discretization: TSD model

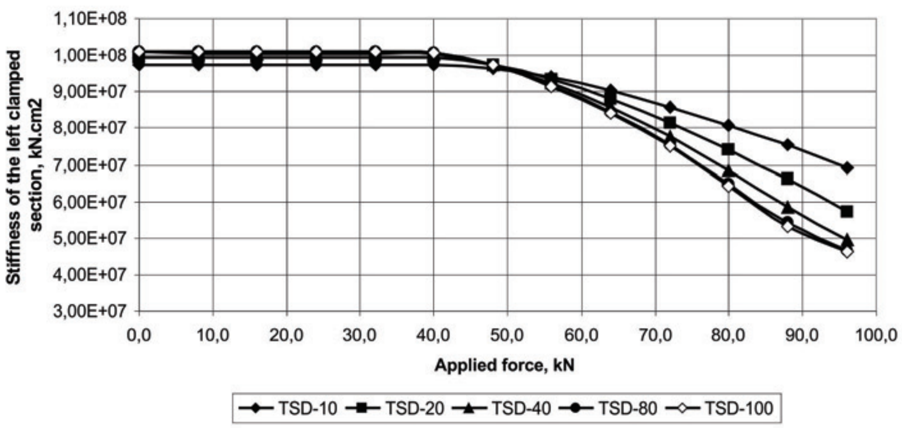

across cracks in concrete nuclear containment vessels. Reinforced concrete structures in seismic zones. Detroit, American Concrete Institute, ACI Special Publication SP-53, 1977; p.203-206.
[08] BAZANT, Z.P.; GAMBAROVA, P.G. Rough cracks in reinforced concrete. Journal of the Structural Division, ASCE, v.106, n.4, April, 1980; p.819-842.
[09] MILLARD, S.G.; JOHNSON, R.P. Shear transfer across cracks in reinforced concrete due to aggregate interlock and to dowel action. Magazine of Concrete Research, v.36, n.126, 1984; p.9-21.
[10] MARTÍN-PEREZ, B.; PANTAZOPOULOU, S.J. Effect of bond, aggregate interlock, and dowel action on the shear strength degradation of reinforced concrete. Engineering Structures, v.23, 2001; p.214-227.
[11] HE, X.G.; KWAN, K.H. Modelling dowel action of reinforcement bars for finite element analysis of concrete structures. Computers and Structures, v.79, 2001; p.595-604.
[12] EL-ARISS, B. Behavior of beams with dowel action. Engineering Structures, v.29, 2007; p.899-903.
[13] SANCHES JR, F.; VENTURINI, W.S. Damage modelling of reinforced concrete beams. Advances in Engineering Software, v.38, 2007; p.538-546.
[14] OLIVER, J.; LINERO, D.L.; HUESPE, A.E.; MANZOLI, O.L. Two-dimensional modeling of material failure in reinforced concrete by means of a continuum strong discontinuity approach. Computer Methods in Applied Mechanics and Engineering, v.197, 2008; p.332-348.
[15] NICKEL, R.E.; SECOR, G.A. Convergence of consistently derived Timoshenko beam finite elements. Int. J. Num. Meth. Eng., v.5, 1972; p.243-253.
[16] PRATHAP, G.; BHASHYAM, G.R. Reduced integration and the shear-flexible beam element. J. Num. Meth. Eng., v.18, 1982; p.195-210.
[17] HEYLIGER, P.R.; REDDY, J.N. A higher order beam finite element for bending and vibration problems. Journal of sound and vibration, v.126, n.2, 1988; p.309-326.
[18] MAZARS, J. Application de la mechanique de l'endommagement au comportement non lineaire et à la rupture du béton de structure, Paris, 1984, Thèse de Doctorat d'État, Université Paris 6.
[19] NOGUEIRA, C.G. Desenvolvimento de modelos mecânicos, de confiabilidade e de otimização para aplicação em estruturas de concreto armado. São Carlos, 2010, Tese (doutorado) - Escola de Engenharia de São Carlos, Universidade de São Paulo, 345 p.
[20] KACHANOV, L.M. Time of rupture process under creep conditions. Izvestia Akademii Nauk, USSR (em russo), n.8; 1958, p.26-31.
[21] LEMAITRE, J.; CHABOCHE, J.C. Mechanique des materiaux solides. Paris, Dunod-Bordas; 1985.
[22] BOTTA, A.S. Cálculo de esforços e deslocamentos em estruturas reticuladas considerando a mecânica do dano no continuo para a modelagem do concreto armado. São Carlos, 1998, Dissertação (mestrado) - Escola de Engenharia de São Carlos, Universidade de São Paulo, 98 p.
[23] PITUBA, J.J.C. Estudo e aplicação de modelos constitutivos para o concreto, fundamentados na mecânica do dano contínuo. São Carlos, 1998, Dissertação (mestrado) - Escola de Engenharia de São Carlos, Universidade de São Paulo, 130 p.
[24] PAULA, C.F. Contribuição ao estudo das respostas numéricas não-lineares estática e dinâmica de estruturas reticuladas planas. São Carlos, 2001, Tese (doutorado) - Escola de Engenharia de São Carlos, Universidade de São Paulo, 128 p.
[25] ÁLVARES, M.S. Estudo de um modelo de dano para o concreto: formulação, identificação paramétrica e aplicação com o emprego do método dos elementos finitos. São Carlos, 1993, Dissertação (mestrado) - Escola de Engenharia de São Carlos, Universidade de São Paulo, 123 p.
[26] ARAÚJO, F.A. Formulação de um modelo de dissipação concentrada para análise não-linear de estruturas reticuladas planas em concreto armado. São Carlos, 2007, Tese (doutorado) - Escola de Engenharia de São Carlos, Universidade de São Paulo, 232 p.
[27] OWEN, D.R.J.; HILTON, H. Finite elements in plasticity. Swansea, U.K, Pineridge Press; 1980.
[28] PROENÇA, S.P.B. Sobre modelos matemáticos do comportamento não-linear do concreto: análise crítica e contribuições. São Carlos, 1988, Tese (doutorado) - Escola de Engenharia de São Carlos, Universidade de São Paulo, 330 p.
[29] BELARBI, A.; HSU, T.T.C. Stirrup stresses in reinforced concrete beams. ACI Structural Journal, September-October, 1990; p.530-538.
[30] SOROUSHIAN, P.; OBASEKI, K.; ROJAS, M.C. Bearing strength and stiffness of concrete under reinforcing bars. ACI Materials Journal, v.84, n.3, May-June, 1987; p.179-184.
[31] NEVES, R.A. Cálculo de esforços e deslocamentos em estruturas de pisos de edifícios considerando-se a influência das tensões cisalhantes. São Carlos, 2000, Dissertação (mestrado) - Escola de Engenharia de São Carlos, Universidade de São Paulo, 132 p.